

COHERENT WAVE-FIELDS FROM RANDOM NOISE IN OCEAN ACOUSTICS AND GEOPHYSICS

W. A. Kuperman, P. Gerstoft, P. Roux, K. Sabra
Marine Physical Laboratory of the Scripps Institution of Oceanography
University of California, San Diego, La Jolla, CA 92093-0238, USA

Abstract: Recently it has been shown that coherent time domain Green's functions (TDGF's) can be extracted from ocean and seismic noise. The TDGF emerges from a correlation process between received noise at two points as if either receiver was a source, and the other a field point. As a matter of fact, since an early result was in the ultrasonic regime, this process has been shown to be robust over at least nine orders of magnitude in frequency. Basic theory, simulation and results from an assortment of regimes illustrate the underlying fundamental physics of this phenomenon and potential applications.

1. INTRODUCTION

Recently, a series of papers in acoustics and geophysics have shown that the time domain Green's function (TDGF) between two points can be extracted from noise [1-12]. Retrieving the full TDGF requires a 3-D homogeneous distribution of noise sources. In the ocean, where the noise sources tend to originate from a surface, one retrieves the TDGF time of arrival structure though the arrival amplitudes will not be correct. For brevity, we refer to the TDGF as a function with the correct time of arrival structure in the sense, that it could be used for time of arrival tomography in which amplitudes are not considered. Thus, if we have a receiver some distance from a receiving array, both embedded in a random noise field, coherent wavefronts on the array with the correct time of arrival structure will emerge from a cross-correlation process that accumulates contributions over time from noise sources whose propagation path pass from the point receiver to the array elements. Theoretically, it is actually the time derivative of the noise correlation function (NCF) that yields TDGF between the sensors. This phenomenon has now been observed in ultrasonic noise fields, ocean acoustic noise fields and seismic noise fields. Further, an analogous result has been observed in seismic coda; that is the scattered field following the "ballistic arrival" is a random field such that cross-correlations between sensors of this late arriving diffuse field also yields the TDGF [13].

2. THEORETICAL AND EXPERIMENTAL CONSIDERATIONS

Based on theoretical and experimental results, the relationship between the TDGF between two receivers 1 and 2 , and the time-derivative of the expected value of the NCF $\langle C_{12}(\tau) \rangle$ is:

$$\frac{d\langle C_{12}(\tau) \rangle}{d\tau} \equiv -g(\mathbf{r}_1, \mathbf{r}_2, t) + g(\mathbf{r}_2, \mathbf{r}_1, -t)$$

The terms on the RHS are respectively: (1) the TDGF which comes from noise events that propagate from receiver 1 to 2 and yields a positive correlation time-delay τ and (2) the time-reversed TDGF which comes from noise events that propagate from receiver 2 to 1 and yields a negative correlation time-delay $-\tau$ (see Fig.1 which includes a shallow water data example of correlation between elements of an array). Thus, for a uniform noise source distribution or a fully diffuse noise field, the derivative of the NCF is an anti-symmetric function with respect to time, the NCF itself being symmetric function.

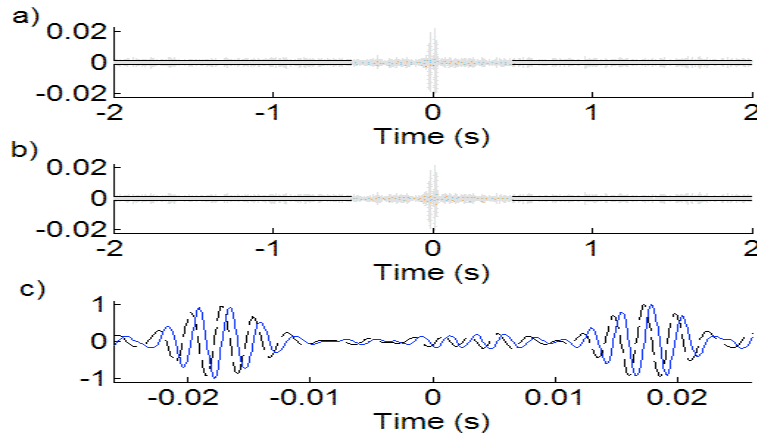


Fig. 1: a) Ambient noise cross-correlation function between two elements of a horizontal bottom array separated by 28m. Thirty-three minutes of ambient noise recordings in the frequency band $B_{-}=300\text{--}550$ Hz were used. The amplitude of the square root of the variance, measured between 0.5 and 2s, is indicated by the black lines. b) Time derivative of the same NCF which can be used to estimate the arrival time structure of the Green's function. c) Zoom around the positive and negative arrival times to compare the two time series: the negative time derivative of the NCF (solid line) is the NCF itself (dashed line)

Note that in Fig. 1c the waveforms are similar but with a phase shift (for narrowband signals) corresponding here to a small time-delay of 0.5ms which yields an error estimate in separation distance of 0.75m. For station pair separated by large distances with respect to the wavelength, thus yielding large arrival-times, this small time delay is often insignificant and within the error bound associated with travel-time measurements. However for small distances, e.g. 28m in this case or roughly 7.5 wavelengths, this small time-delay can cause a significant error in travel-time measurements. Thus, using the derivative of the NCF yields a crucial difference for the precise measurement required for array element localization [8] or small scales tomography

3. PHYSICAL EXPLANATION OF THE NOISE CORRELATION PROCESS USING A DEEP WATER EXPERIMENT

We have used data from a deep water experiment collected by the NPAL group to accumulate noise and demonstrate that the NCF yields the TDGF. Even for large scale

shipping noise we have shown that the correct time of arrival structure emerges. Figure 2 is both a schematic and data demonstrating the whole process. Under such conditions, though, the NCF more often tends to be one sided because of the geographical distribution of the shipping lanes.

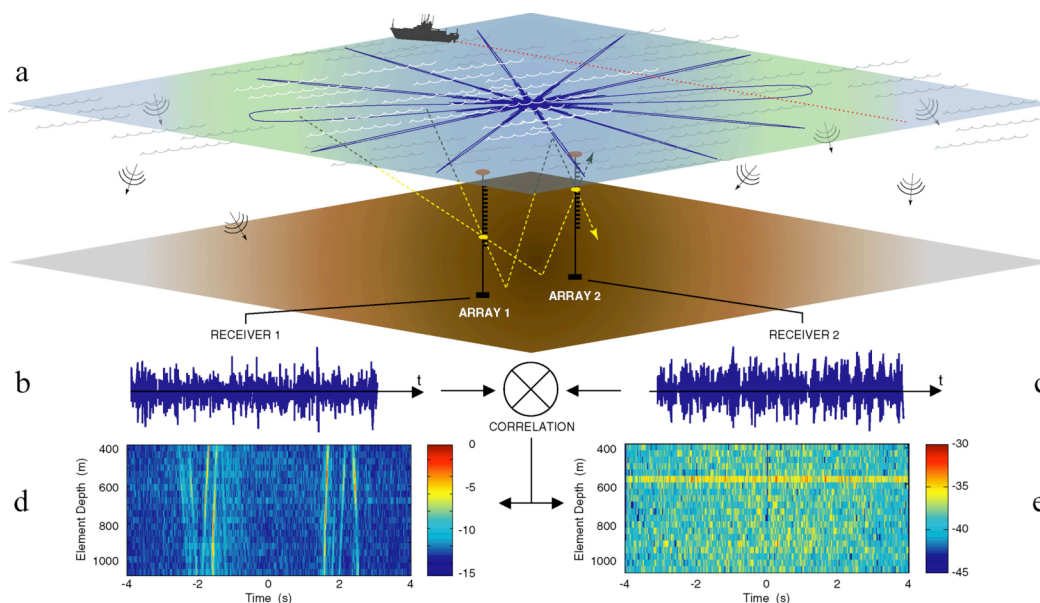


Fig. 2: (a) Two arrays are depicted at a separation distance R . A schematic of the directivity pattern of the time-domain correlation process between two receivers on each array is projected on the ocean surface. Only a discrete set of lobes have been displayed that correspond to noise sources whose emission angle is equal to -60° , -30° , 0° , 30° , 60° and 90° . Each angular lobe depends on the central frequency and bandwidth and corresponds to a delay time in the correlation function. For the case of equally distributed ambient noise sources, the broad endfire directions will contribute coherently over time to the arrival times associated with the TDGF while the contribution of the narrow off-axis sidelobes will average down. For the case of shipping noise, coherent wavefronts emerge only when there is sufficient intersection of the shipping paths with the endfire beams. However, if there is a particular loud shipping event, it will dominate so that either impractically long correlation times are needed, or discrete events should be filtered out. (b) and (c) The correlation process is done using time-domain ambient noise simultaneously recorded on two receivers in array 1 and 2. (d) Spatial temporal representation of the wavefronts obtained from the correlation process between a receiver in array 1 at depth 500 m and all receivers in array 2 separated by a distance $R=2200$ m. The arrival structure of the correlation function is composed of the direct path, surface reflected, bottom reflected, etc. as expected in the TDGF. The correlation function is plotted in a dB scale and normalized by its maximum. (e) The same correlation processing is performed on data that have not been recorded at the same time on the two arrays. In (d) and (e), the x and y-axis correspond to the time axis of the cross-correlation function and receiver depth, respectively. The correlation functions are plotted in a dB scale and normalized by the maximum of (d)

In the above example, only short segments of data were available so the issue of time necessary to build up a complete TDGF is not addressed in this data set.

4. EMERGENCE TIME FOR THE TDGF FROM THE NOISE

We have used data from the shallow water example mentioned in Section 2 to compare with simple theory of the emergence of the TDGF. The emergence rate can be defined based on the variance of the NCF and an analytical expression of the variance of the NCF can be derived independently of the particular expression of the Green's function. The resulting analytic formula for variance of the NCF is derived assuming only 1) an isotropic distribution of impulsive random noise sources and 2) a finite duration Green's function which is true for any physical systems in the presence of attenuation:

$$[Var(C_{12}(\tau))]_{\tau > T_{disp}} = \frac{\langle C_{11}(0) \rangle \langle C_{22}(0) \rangle}{2B_{\omega} T_r} = \frac{\int_0^{T_r} P_1^2(t) dt \int_0^{T_r} P_2^2(t) dt}{2B_{\omega} T_r}$$

This simplified expression of the variance is a constant proportional to the product of the total recorded energy by each receiver (which includes the receiver response, noise source amplitude, and potential site effects) and inversely proportional to the recorded time-bandwidth product [14].

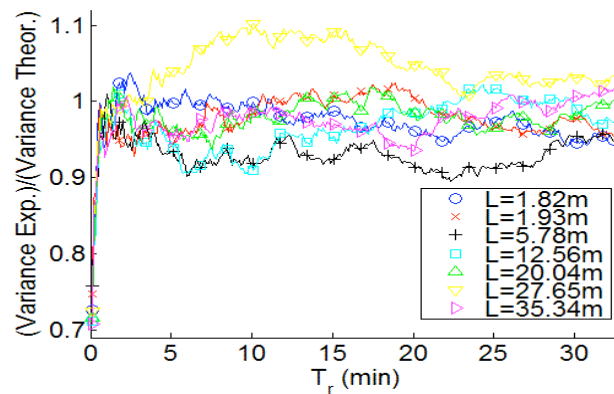


Fig. 3: For the array of Fig. 1, we plot the ratio of the experimental measurements of the variance and the simplified theoretical predictions for the variance of the NCF with increasing separation distance L from 1.82m to 27.65m

The variance of the NCF was computed for long time-delay $0.5s < \tau < 2s$, much larger than the maximal travel time between array element which is $(N-1)D/c \approx 0.08s$, where $N=64$, $D=1.875m$, and $c=1500m/s$. For instance, the square root of the variance is indicated by a thick line for respectively the NCF and its time-derivative on Fig. 1.a and Fig. 1.b, corresponding to a receiver separation distance of 28m and a recording time $T_r = 33min$. The experimental variance of the NCF, based on the experimental NCF in Fig 1.a, was computed for 6 receivers pairs spaced from 1.82m to 27.65m (using element 30 as the first receiver and by using different hydrophones as the second receivers) for increasing recording time from

6.6sec to 33min by increment of 6.6s between 350Hz and 550Hz. Figure 3 compares the ratio of the experimental measurements of the variance of the NCF and the theoretical predictions for the variance of the NCF for increasing recording time T_r and for each of the 6 receiver pairs. The ratio remains close to one for all receiver pairs and recording time T_r larger than 1 minute. The theoretical predictions deviate from the experimental results for a small recording time-window length T_r (below 1min here), that is insufficient for the time-averaging for the ambient noise statistics to converge. Furthermore, the deviations of the noise source distributions from the case of an isotropic distribution may also affect the results.

5. A GEOPHYSICS EXAMPLE

We give here an example of tomography using seismic data in which the medium variability is not an issue. We correlate data from a set of seismic stations pairs (see +’s Fig. 4c) over a period of 30 days, take the time derivative. Figure 4b plots the seismic vertical components ordered in terms of pair separation. This data was then inverted by a simple tomographic procedure for the surface shear speed in this region; a map of the results is shown in Fig.4c in agreement with known results obtained over many years of seismic exploration and research.

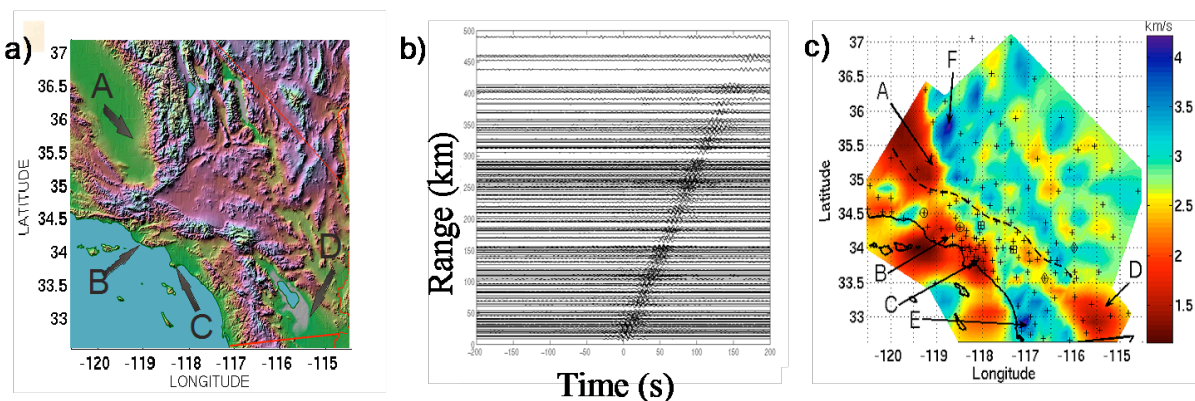


Fig. 4: Inversion from noise. a) Topographic map of Southern California. Low altitude sedimentary basins (green color), are indicated by the arrows (A: San Joaquin Valley, B: Ventura, C: Los Angeles, D: Salton Trough). b) The NCF time derivatives for station pair separations of up the 500 km. c) Seismic stations (+) distributed over Southern California on top of the tomographic inversion for surface speed. A comparison with a topographic map (shown in a)) shows a good correspondence between the main geological features of the Southern California. The main regions with slow surface-wave velocity (below 2 km/s) are related to the same large sedimentary basins as indicated in a). Fast group velocities characterize mountain ranges (E: Peninsular Ranges and F: Sierra Nevada)).

6. CONCLUSION

The use of ambient noise to extract the properties of deterministic propagation conditions in acoustic and elastic media has been demonstrated. This method provides the basis for passive tomography and other inversion schemes. A growing body of inversion research results, such as the implementation of a passive fathometer [15] based on adding a beamformer to the noise correlation method, promises to provide further utility of heretofore nuisance noise fields.

REFERENCES

- [1] Weaver, R.L., and O.I. Lobkis, Ultrasonics without a Source: Thermal Fluctuation Correlations at MHz Frequencies, *Phys. Rev. Lett.*, **87**, 134301 (2001),
- [2] Roux, P., W.A. Kuperman, and the NPAL Group Extracting coherent wavefronts from acoustic ambient noise in the ocean, *J. Acoust. Soc. Am.*, **116**, 1995—2003 (2004),
- [3] Roux, P., K.G. Sabra, W.A. Kuperman and A. Roux, Ambient noise cross-correlation in free space: theoretical approach, *J. Acoust. Soc. Am* **117**, 79—84 (2005).
- [4] Sabra, K.G., P. Roux, and W.A. Kuperman, Arrival-time structure of the time-averaged ambient noise cross-correlation function in an oceanic waveguide, *J. Acoust. Soc. Am.*, **117** 164—174. (2005).
- [5] Campillo, M. and A. Paul, Long-range correlations in the diffuse seismic coda, *Science*, **299**, 547-549 (2003),
- [6] Weaver, R.L., and O.I. Lobkis, Elastic wave thermal fluctuations, ultrasonic waveforms by correlation of thermal photons, *J. Acoust. Soc. Am*, **113**, 2611--2621. (2003).
- [7] Wapenaar, K., Retrieving the Elastodynamic Green's Function of an Arbitrary Inhomogeneous Medium by Cross Correlation, *Phys. Rev. Lett* **93**, 254301. (2004).
- [8] Sabra, K.G., P. Roux, A.M. Thode, G.L. D'Spain, W.S. Hodgkiss, and W.A. Kuperman, Using ocean ambient noise for array self-localization and self-synchronization. Submitted to *IEEE J. Oceanic Eng*, **30** (2), 338- 347 (2005).
- [9] Sabra, K.G., P. Gerstoft, P. Roux, W.A. Kuperman and M. C. Fehler Extracting time-domain Greens function estimates from ambient seismic noise,, *Geophys. Res. Lett.* **32**, L03310 (2005),
- [10] Sabra, K.G., P. Gerstoft, P. Roux, W.A. Kuperman and M. C. Fehler, Surface wave tomography from seismic ambient noise in Southern California, *Geophys. Res. Lett.* **32**, doi:10.1029/2005GL023155 (2005).
- [11] Shapiro, N.M. and M. Campillo Emergence of broadband Rayleigh waves from correlations of the ambient seismic noise, *Geophys. Res. Lett.*, **31** L07614. (2004).
- [12] Shapiro, N.M. , M. Campillo, Laurent Stehly and Michael H. Ritzwoller High resolution surface wave tomography from ambient seismic noise, *Science.*, **307**, 1615-1618, (2005).
- [13] Campillo, M. and A. Paul (2003), Long-range correlations in the diffuse seismic coda, *Science*, **299**, 547-549
- [14] Sabra, K.G., P. Roux, W.A. Kuperman, Emergence rate of the time-domain Greens function from the ambient noise cross-correlation function, *J. Acoust. Soc. Am*, **118**, pp. 3524-3531 (2005).
- [15] Siderius, M, Porter, M. B., and Harrison, C. , An Passive fathometer for determining bottom depth and imaging seabed layering using ambient noise. *J. Acoust. Soc. Am.*, in press (2006).